Fish and Shellfish Immunology 134 (2023) 108629

Contents lists available at ScienceDirect

Fish and Shellfish Immunology

journal homepage: www.elsevier.com/locate/fsi

Full length article

Molecular characterization and immune response of suppressor of cytokine signaling 5b from redlip mullet (*Planiliza haematocheilus*): Disclosing its anti-viral potential and effect on cell proliferation

H.M.S.M. Wijerathna [a], Kishanthini Nadarajapillai [a], K.A.S.N. Shanaka [a], T.D.W. Kasthuriarachchi [a], Sumi Jung [a,b], Seongdo Lee [c], Jehee Lee [a,b,*]

[a] *Department of Marine Life Sciences & Fish Vaccine Research Center, Jeju National University, Jeju, 63243, Republic of Korea*
[b] *Marine Science Institute, Jeju National University, Jeju, 63333, Republic of Korea*
[c] *National Fishery Product Quality Management Service, Busan, 49111, Republic of Korea*

ARTICLE INFO

Keywords:
Planiliza haematocheilus
Suppressors of cytokine signaling 5b
Anti-Viral potential
Cell proliferation

ABSTRACT

The suppressor of cytokine signaling (SOCS) proteins family comprising eight proteins (SOCS1-7 and cytokine-inducible SH2-containing (CIS)) are classical feedback inhibitors of cytokine signaling. Although the biological role of CIS and SOCS1-3 have been extensively studied, the biological functions of SOCS4-7 remain unclear. Here, we elucidated the molecular characteristics, expression profile, immune response, anti-viral potential, and effect on cell proliferation of Phsocs5b, a member of the SOCS protein family from redlip mullet (*Planiliza haematocheilus*); *phsocs5b* comprised 1695 nucleotides. It was 564 amino acids long with a molecular weight of 62.3 kDa and a theoretical isoelectric point of 8.95. Like SOCS4-7 proteins, Phsocs5b comprised an SH2 domain, SOCS box domain, and a long N-terminal. SH2 domain is highly identical to its orthologs in other vertebrates. Phsocs5b, highly expressed in the brain tissue, was localized in the cytoplasm. Temporal changes in *phsocs5b* expression were observed following immune stimulation with polyinosinic: polycytidylic acid, lipopolysaccharide, and *Lactococcus garvieae*. In FHM cells, Phsocs5b overexpression suppressed the viral hemorrhagic septicemia virus (VHSV) infection and epidermal growth factor receptor (*egfr*) expression but increased the mRNA levels of *pi3k, akt,* pro-inflammatory cytokines (*il1β* and *il8*), and anti-viral genes (*isg15* and *ifn*). Overall, our findings suggest that Phsocs5b attenuates VHSV infection, either by hindering the cell entry via degradation of Egfr, enhancing pro-inflammatory cytokines and anti-viral factor production, or both. The results also indicated that Phsocs5b could directly activate Pi3k/Akt pathway by itself, thus enhancing the proliferation and migration of cells. Taken together, Phsocs5b may be considered a potential therapeutic target to enhance immune responses while positively regulating the proliferation and migration of cells.

1. Introduction

The suppressors of cytokine signaling (SOCS) family proteins have been identified as feedback inhibitors of cytokine signaling [1]. Eight SOCS family members have been discovered in mammals, including SOCS1-7 and cytokine-inducible Src homology 2 (SH2)-containing protein (CIS) [2]. All SOCS family proteins comprise a low-conserved N-terminal domain with varying lengths, a conserved central SH2-domain, and a carboxy C-terminal with a 40-amino acid motif known as the SOCS box domain [3]. The SH2-domain of SOCS proteins can bind to the phosphorylated tyrosine residues on the activated receptor/Janus kinase (JAK) complex, which is important for cytokine-mediated signal transduction via Janus kinase-signal transducer and activator of transcription (JAK-STAT) pathway, and subsequently, inhibit the signal transduction by hindering the access of other signaling molecules or directly inhibiting the activity of JAK [4,5]. The SOCS box domain plays a role in polyubiquitylation and the subsequent proteasomal degradation of substrate proteins [6]. However, each of these SOCS5 proteins acts via specific mechanisms. SOCS1 and SOCS3 contain a kinase inhibitory region, which inhibits the catalytic activity of JAK tyrosine kinase together with the SH2 domain [7,8]. CIS and SOCS1-3 are stimulated by cytokines, and its negative feedback

* Corresponding author. Marine Molecular Genetics Lab, Jeju National University, 102 Jejudaehakno, Jeju, 63243, Republic of Korea.
E-mail address: jehee@jejunu.ac.kr (J. Lee).

https://doi.org/10.1016/j.fsi.2023.108629
Received 14 August 2022; Received in revised form 27 January 2023; Accepted 19 February 2023
Available online 21 February 2023

mechanism inhibits the same cascade, which induces their production [2,9–11]. They compete with STAT to bind the phosphorylated tyrosine residue on the cytoplasmic domains of the receptors of the JAK-STAT pathway [12]. Even though all the SOCS family proteins show common domain organization, SOCS4-7 proteins have a relatively long, less conserved N-terminal region [3]. However, whether SOCS4-7 impact cytokine secretion and their mechanisms of action are unclear [2,12].

Several studies have investigated the role of SOCS5 in mammals. Seki et al. reported that mammalian SOCS5 negatively regulates interleukin 4 (IL-4)-dependent activation of STAT6 and T-helper 2 (TH2) cell differentiation [13]. Sanchez-Mejias et al., for the first time, explained the role of the SOCS5/miR-18a/miR-25 axis in mammals to regulate the tumor suppressor TSC1 followed by mTOR signaling and the potential therapeutic use of inhibition of miR-18a and miR-25 to restore SOCS5 levels in hepatocellular carcinoma to suppress liver cancer [14]. Another study demonstrates that miR-151a-3p targets SOCS5 to enhance postmenopausal osteoporosis by activating JAK2/STAT3 signaling [15]. Furthermore, SOCS5 interacts with the epidermal growth factor receptor (EGFR) to degrade and eliminate it from the cell surface [16]. Kedzierski et al. showed that the degradation of EGFR reduces influenza A virus (IAV) infection in airway epithelium [17]. EGFR triggers the activation of the phosphoinositide-3 kinase (PI3K)/serine-threonine protein kinase (AKT) pathway, which is important in cell migration and survival [18]. However, studies on the functions of SOCS family proteins, particularly the SOCS5 ortholog, in teleost are scarce [19].

Redlip mullet (*Planiliza haematocheilus*), a teleost (Mugiliformes, Mugilidae), also known as so-iuy mullet, is mostly spread along the entire coast of Korea [20]. Mullets are economically valuable species and account for 9.3% of the total aquaculture fish supply in South Korea in 2021 [21]. They are used as raw fish in South Korea and as dried salted fish roe in some other countries, including the southeastern United States, Taiwan, and Japan [22]. Redlip mullets are commercially cultured mainly along the south coast of South Korea as food fish. However, mullet cultivation became difficult due to its high mortality rate, but the reason for this is still unclear [20]. Very few studies have studied the *Amyloodinium* sp. and *Myxobolus* sp. infections in mullets in South Korea [22,23]. Nevertheless, it is important to identify and explore the functions of immune-related molecules in redlip mullet to provide a holistic solution for the cultivation of this commercial fish species. Therefore, in the present study, we aimed to characterize the structure and function of SOCS5b ortholog from redlip mullet. We also investigated the regulatory effect of Phsocs5b on the immune response against cytokine stimulants and cell migration and survival.

2. Materials and methods

2.1. Bioinformatic analysis of Phsocs5b

Phsocs5b coding sequence was identified from a previously established redlip mullet transcriptome database and confirmed using the National Center for Biotechnology Information (NCBI) Basic Local Alignment Search Tool (BLAST) [24]. Unipro UGENE software (Version 41.0) was used to predict the open reading frame (ORF) and the amino acid sequence of Phsocs5b [25]. Simple modular architecture research tool (SMART) program [26] and the NCBI conserved domain search tool [27] were used to infer potential domains, motifs, and signal peptides. Phsocs5b structure was predicted with Iterative Threading ASSEmbly Refinement (I-TASSER) server [28]. Then, the predicted 3D structure was visualized and edited using the PyMOL Molecular Graphic System Version 2.5.1 [29]. Multiple sequence analysis of *phsocs5b* was done with other vertebrate orthologs using the Clustal Omega multiple sequence alignment tool [30] and the sequence manipulation suite (SMS): color align conservation tool (https://www.biologicscorp.com/sms2/color_ align_cons.html). Furthermore, pairwise sequence analysis was performed with EMBOSS Needle pairwise sequence alignment tool [31]. The phylogenetic tree was constructed using the MEGA (version 11) software (5000 bootstrap replicates and neighbor-joining method) [32].

2.2. Cloning of the ORF into expressional plasmids

Gene-specific PCR primers were designed with appropriate restriction sites to construct the inserts with the coding sequence for *phsocs5b* using the ORF of the laboratory redlip mullet cDNA library as the template. The amplified gene was cloned into the pcDNA 3.1 (+) (Invitrogen, Carlsbad, CA, USA) and pEGFP-N1 (Invitrogen) expression vectors to construct the pcDNA 3.1(+)-*phsocs5b* and pEGFP-N1-*phsocs5b* plasmids, respectively. Successful cloning was confirmed by sequencing (Macrogen, Korea).

2.3. Cell culture and plasmid transfection

Fathead minnow (FHM) cell line was maintained in Leibovitz L-15 culture medium (Sigma-Aldrich, St. Louis, MO, USA) with 1% antibiotic-antimycotic (Gibco-BRL; Life Technologies) and 10% heat-inactivated fetal bovine serum (FBS, Gibco-BRL; Life Technologies, Carlsbad, CA, USA) as a supplement at 25 °C in an incubator. Plasmid transfection into FHM cells was performed using the X-tremeGENE™ 9 transfection reagent (Roche Diagnostics GmbH, Penzberg, Germany) following the manufacturer's protocol.

2.4. Phsocs5b subcellular localization

To observe the subcellular localization of Phsocs5b, a 12-well cell culture plate was seeded with FHM cells (2×10^5 cells/well) and incubated at 25 °C for 12 h. Subsequently, 1 μg pEGFP-N1 vector or pEGFP-N1-*phsocs5b* plasmid constructs were transfected into the cells cultured in 1 mL cell culture medium. After 24 h, overexpressed cells were washed with 1 × phosphate-buffer saline (PBS) and incubated for 10 min with 4% formaldehyde for fixation. Then, the cells were treated with 4,6-diamidino-2-phenylindole (DAPI) (Invitrogen) and Cytopainter Phalloidine-iFluor 594 staining solution (Abcam, UK) according to the manufacturer's instructions to stain the nucleus and F-actin in the cytoplasm of the cells and incubated for 30 min at 25 °C. After that, the cells were washed with 1 × PBS and observed under the fluorescence microscope at 400 × magnification (Leica DM6000 B; Leica Microsystems, Wetzlar, Germany). Leica Application Suite X (version 3.3) software was used to process the captured images.

2.5. Experimental animal tissue isolation and transcriptomic database construction

All the *in vivo* experiments were conducted with the approval of the Jeju National University animal experiment ethics committee (Approval no: 2018-003). Redlip mullets with an average body weight of 100 g were purchased from Sangdeok Fishery fish farm in Handong, Republic of Korea. The fish were acclimatized in a 400 L aquarium tank at 20 ± 1 °C with sea water (pH 7.6, salinity 34 ± 1%, and 14:10 h light/dark cycle) for two weeks before the experiments. The redlip mullets were fed commercial fish feed twice per day, and their health condition during the acclimatization was determined in accordance with the guidelines for the health and welfare monitoring of experimental fish [33].

After a two-week-acclimatization period, healthy fish were anesthetized using 40 mg/L tricaine mesylate (MS222, Sigma-Aldrich, USA) to analyze the tissue-specific mRNA expression. Five redlip mullets were dissected, and the liver, spleen, head kidney, gill, kidney, intestine, skin, heart, muscle, and stomach tissues were isolated. Blood collection was done using heparin sodium salt (USB, USA)-coated syringes and centrifuged immediately at 3000×*g* and 4 °C for 10 min to precipitate the peripheral blood cells. All samples were snap frozen and stored at −80 °C until RNA extraction.

Pacific Biosciences (PacBio) sequencing technology was used to

Table 1
Primer sequences used in cloning and qPCR analysis.

Primer name	Sequence (5`-3`)	Application
PhSOCS5b_pcDNA (Forward)	GAGAGAaagcttGCACCATGAAGAAAGCGGGCAACATG (*Hind*III)	Cloning into pcDNA3.1(+)
PhSOCS5b _pcDNA (Reverse)	GAGAGAtctagaCTATTTGACCTTGAGTGGCGGTTC (*Xba*I)	
PhSOCS5b _pEGFP (Forward)	GAGAGAaagcttACCATGAAGAAAGCGGGCAACATG (*Hind*III)	Cloning into pEGFP-N1
PhSOCS5b _pEGFP (Reverse)	GAGAGAggtaccGCTTTGACCTTGAGTGGCGGTTC (*Kpn*I)	
PhSOCS5b _qPCR (Forward)	GGCACTTGATCAAACAACACACAGC	qPCR analysis
PhSOCS5b _qPCR (Reverse)	CACACCTTCCTCGATGCTAAGTCG	
VHSV G protein _qPCR (Forward)	TACAACATCACCCTGCCCAACC	To analyze VHSV amplification
VHSV G protein _qPCR (Reverse)	GACCACCCTGTGATCATGTGTCC	
VHSV P protein _qPCR (Forward)	CGACAACATACTCTCCATCC	To analyze VHSV amplification
VHSV P protein _qPCR (Reverse)	CCAAGTGCTCTCTCATTCC	
VHSV N protein _qPCR (Forward)	TGTCTCAGATCAGTGGGAAGTACGC	To analyze VHSV amplification
VHSV N protein _qPCR (Reverse)	GGACCTCAGCGACAAGTTCGG	
VHSV R protein _qPCR (Forward)	CAAGTGCGGACACGATCAATCCC	To analyze VHSV amplification
VHSV R protein _qPCR (Reverse)	TGAGGAAAGGGCAACCATTCGC	
Pi3k_qPCR (Forward)	AGCCAAGACTCTCCACACTATACGG	To analyze expression in FHM cells
Pi3k_qPCR (Reverse)	GTCAGCATGTCTTCAGGAAGATCCC	
Akt_qPCR (Forward)	GACCGGTTGTGTTTCGTCATGGAG	To analyze expression in FHM cells
Akt_qPCR (Reverse)	TTTCGCTCCGCATGCAGGTAATC	
EGFR_qPCR (Forward)	ACTGGCCTAAACACCTCAAATCCC	To analyze expression in FHM cells
EGFR_qPCR (Reverse)	TCACTGATCTCCTTCAACGAACGC	
IL-1β_qPCR (Forward)	AGACCAATCTCTACCTCGCTTGTAC	To analyze expression in FHM cells
IL-1β_qPCR (Reverse)	TTAATGGTGTTTAATGTTTCACTGATCTC	
IL-8_qPCR (Forward)	CCCTCCTAGCCCTCACTGTAAA	To analyze expression in FHM cells
IL-8_qPCR (Reverse)	GGATCTTCTCAATGACCTTCTT	
IFN_qPCR (Forward)	AAGAATGCGTGGCCCAATACCA	To analyze expression in FHM cells
IFN_qPCR (Reverse)	ATCCTCTGAAGGTGGCTTCTCACA	
ISG-15 (Forward)	AATGGAGATGTGAAGCGGCTGGA	To analyze expression in FHM cells
ISG-15 (Reverse)	AACCCGTAACTGCTGAGGCTTCT	
EF1α_qPCR (Forward)	GGCTGACTGTGCTGTGCTGAT	qPCR internal reference of FHM cells
EF1α_qPCR (Reverse)	GTGAAAGCCAGGAGGGCATGT	

construct the mullet transcriptomic database. Total RNA was isolated from the collected tissues of the redlip mullet fish and sent to Insilicogen, Korea, for sequencing and cDNA library construction [34].

2.6. In vivo immune challenge

To understand the response of Phsocs5b upon pathogenic stimulations, healthy redlip mullets were injected intraperitoneally with 1.5 μg/g polyinosinic: polycytidylic acid (Poly I:C), 1.25 μg/g lipopolysaccharides (LPS) from *Escherichia coli* 055:B5 (Sigma-Aldrich), and 1×10^3 CFU/μL *Lactococcus gavieae* (Chonnam National University, South Korea) dissolved in 100 μL PBS. Fish injected only with 100 μL PBS were used as control. The bacteria culture was prepared on brain heart infusion media supplemented with 1.5% salt and incubated at 37 °C. After injection, five fish were sampled at each time point (0, 6, 24, 48, and 72 h post-injection [h p.i.]) to isolate the blood cells as described before. Blood cells obtained from five fishes were pooled and stored at −80 °C for RNA extraction.

2.7. Total RNA extraction and quantitative reverse transcription PCR (RT-qPCR)

Total RNA was isolated from the collected tissues of redlip mullet fish and FHM cells using the RNAiso Plus kit (Takara Bio Inc, Shiga, Japan). The isolated RNA was quantified using μDrop Plate (Thermo Fisher Scientific, Waltham, MA, USA) and Multiskan SkyHigh microplate reader (Thermo Scientific, USA). The quality of the RNA was assessed by agarose gel electrophoresis and evaluation of the absorbance values at 260 and 280 nm using a Multiskan SkyHigh microplate reader. cDNA was synthesized from 2.5 μg RNA using the PrimerScript II First Strand cDNA Synthesis Kit (Takara Bio Inc). Expressional analysis was performed using the qPCR method with TB Green® Premix Ex Taq™ (Tli RNaseH Plus; Takara Bio Inc) in a Thermal Cycler Dice™ Real-Time System III, (Model: TP951; Takara Bio Inc). IDT Primer Quest Tool [35] was used to design the qPCR primers, and all the primers used in the experiment are shown in Table 1. The transcription level of *phsocs5b* was calculated using the Livak $2^{-\Delta\Delta CT}$ method [36].

2.8. Virus replication assay, cytokine, and anti-viral gene expression analysis

FHM cells (8×10^5 cells/well in 6-well plates) were transfected with 1 μg/mL pcDNA3.1(+) or pcDNA3.1(+)-*phsocs5b*. After 24 h, cell culture media was changed into reduced serum (5% FBS)-containing medium. The cells were infected at a multiplicity of infection (MOI) of 0.01 with rVHSV-ΔNV-EGFP, kindly provided by the Department of Aquatic Life Medicine and the Department of Marine Biomaterials & Aquaculture, Pukyong National University, Busan, South Korea [37], and incubated at 20 °C.

To investigate the effect of Phsocs5b on VHSV replication in FHM cells, images of the cells expressing green fluorescent protein (GFP) were observed at 12 and 24 h p.i. using a fluorescence microscope (200 × magnification; Leica Microsystems, Wetzlar, Germany). The cells were harvested at 0, 12, 24, and 48 h p.i. and RT-qPCR was performed to analyze VHSV-N protein level, followed by the estimation of virus copy number using a standard curve described by Kim et al. [38]. Moreover, a plaque assay was performed to analyze the virus titer in the cell culture medium of 12 and 24 h samples [39]. In addition, mRNA expression levels of genes encoding VHSV G-, P-, N-, and R-proteins in 24 h p.i. sample were estimated using RT-qPCR.

Furthermore, the effect of Phsocs5b on the mRNA expression levels of pro-inflammatory cytokine (*il1β* and *il8*) and anti-viral genes (*isg15* and *ifn*) upon VHSV infection at 0, 12, 24, and 48 h p.i. were determined using RT-qPCR.

2.9. Analysis of transcription level of egfr and Pi3k/Akt pathway-related genes

FHM cells were seeded in a 12-well cell culture plate (4×10^5 cells/well) and transfected with 1 μg/mL pcDNA3.1(+) or pcDNA3.1(+)-*phsocs5b*. At 24 h p.i., the mRNA expression levels of *egfr*, *pi3k*, and *akt* were measured using RT-qPCR.

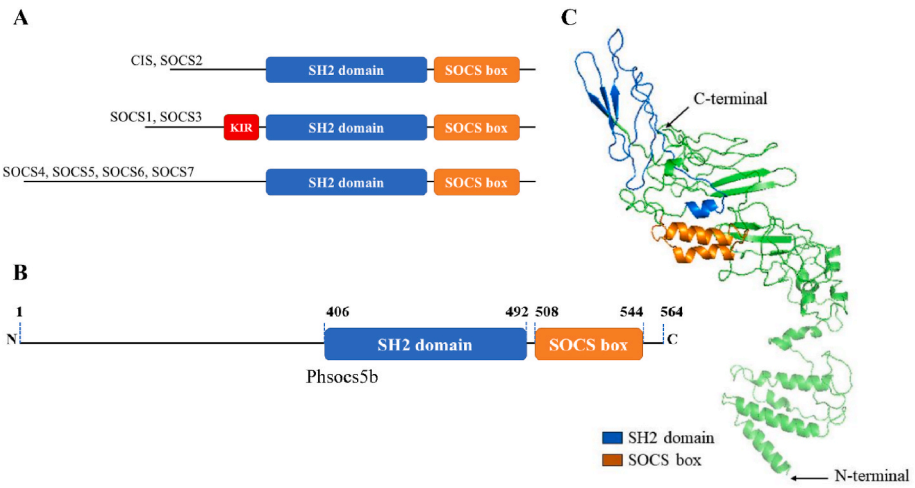

Fig. 1. Schematic structure of SOCS family proteins **(A)**, domain structure **(B),** and predicted 3D tertiary structure **(C)** of Phsocs5b. The domain structure of Phsocs5b was predicted using the online Simple Modular Architecture Research Tool (SMART) EMBL tool. The 3D tertiary structure was predicted from the I-TASSER Server and visualized and edited using the PyMOL software. Phsocs5b comprises 564 amino acids with SH2 domain, SOCS box domain, and long N-terminal. SH2 and SOCS box domains are shown in blue and orange colors, respectively.

2.10. Scratch assay

This experiment was performed to investigate the effect of Phsocs5b on cell proliferation. FHM (6×10^5 cells/well in 12-well cell culture plate) cells were transfected with 1 μg/mL pcDNA3.1(+) or pcDNA3.1 (+)-*phsocs5b* and incubated for ~24 h to obtain a confluent monolayer. Next, a scratch was made using a 200 μL micropipette tip, and detached cells were removed by washing the scratched monolayer with 1 × PBS three times. Then, 10% FBS containing L-15 culture medium was added to the plates. During incubation, cell scratches at different time points (0, 6, 12, 24, 36, and 48 h) were captured using a microscope (100 × magnification; Leica Microsystems, Wetzlar, Germany). The scratched

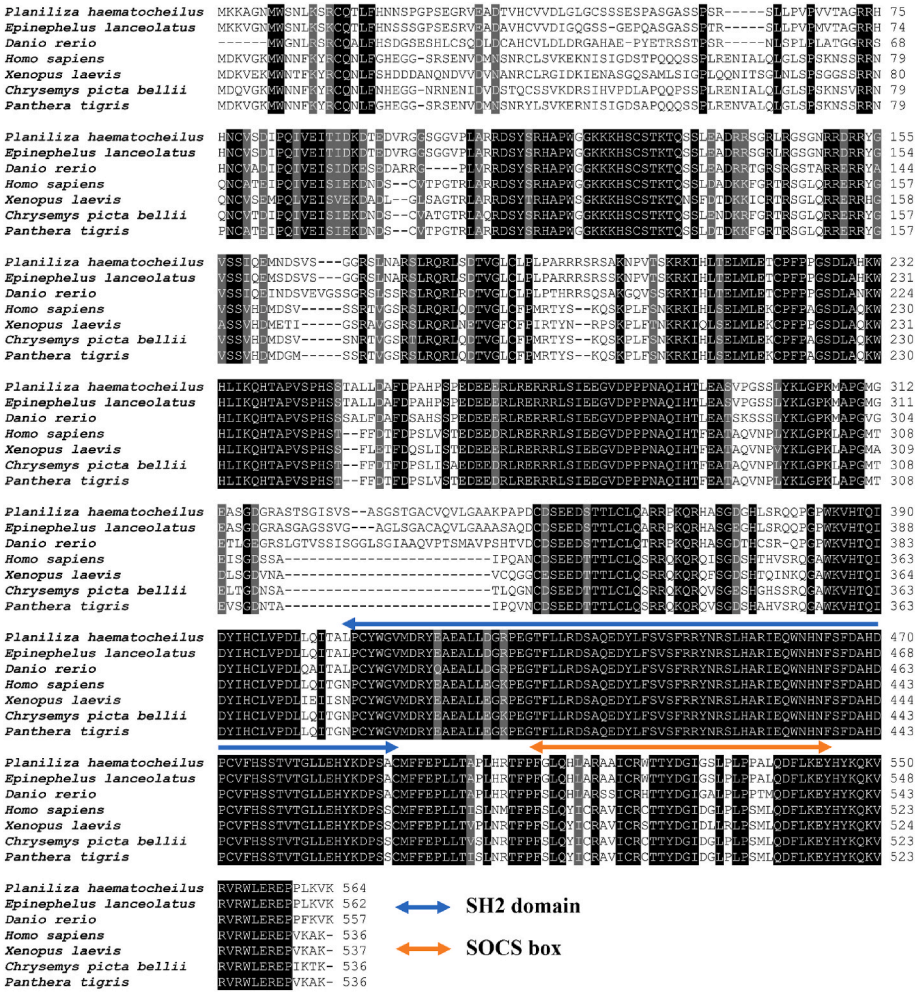

Fig. 2. Multiple sequence alignment of Phsocs5b amino acid sequence (GenBank accession number: ON586847) with its other vertebrate orthologs. Fully and nearly conserved amino acids are shaded in black and gray colors, respectively. The SH2 domain is the highly conserved domain.

Table 2
Pairwise identity and similarity percentages of PhSOCS5b with selected orthologs of other vertebrates.

Species	Accession number	Taxonomy	Identity (%)	Similarity (%)
Epinephelus lanceolatus	XP_033468725.1	Fish	95.0	96.8
Seriola dumerili	XP_022599384.1	Fish	94.7	96.6
Plectropomus leopardus	XP_042357619.1	Fish	95.0	96.5
Scophthalmus maximus	XP_035461699.1	Fish	93.4	96.3
Panthera tigris	XP_042837259.1	Mammalia	65.0	73.8
Orycteropus afer	XP_042637406.1	Mammalia	65.4	74.3
Dipodomys spectabilis	XP_042531382.1	Mammalia	65.3	74.1
Chrysemys picta bellii	XP_042711103.1	Reptilia	65.2	74.0
Sceloporus undulatus	XP_042301480.1	Reptilia	63.6	72.4
Xenopus laevis	XP_041420218.1	Amphibia	62.3	72.5
Bufo	XP_040286250.1	Amphibia	64.5	74.1
Rana temporaria	XP_040207503.1	Amphibia	62.3	73.5

area was measured using the Digimizer image analysis software (Version 5.4.4) to quantify cell proliferation efficiency.

2.11. Statistical analysis

All the experiments were performed in triplicate. The results are presented as the mean ± standard deviation (SD). Tissue distribution results were statistically evaluated using one-way analysis of variance (ANOVA). The statistical significance of the differences between the groups was evaluated using Student's *t*-tests. The GraphPad Prism (Version 8.0.2) software (GraphPad Software, Inc., San Diego, CA, USA) was used to plot the graphs. A p-value of < 0.05 was considered significant.

3. Results and discussion

3.1. Bioinformatic analysis of Phsocs5b

The sequence of *phsocs5b* has been submitted to the NCBI GeneBank under the accession number: ON586847. This study estimated the length of phsocs5b as 1695 bp, and the encoded protein comprised 564 amino acids with a molecular weight of 62.3 kDa. As the isoelectric point (pI) value depends on the amino acid composition of the respective protein [40], we estimated the theoretical pI using the amino acid sequence data. The calculated pI value indicates that Phsocs5b has a net zero charge at 8.95 pH. A schematic representation of the SOCS family of proteins is shown in Fig. 1A [2]. The predicted domain structure and the 3D structure of Phsocs5b are shown in Fig. 1B and C. The predicted 3D structure of Phsocs5b with the highest C-score (−1.18), estimated using the I-TRASSER-server, was selected. The confidence of the predicted structure was assessed by considering the C-score ranges from −5 to 2; a higher C-score value indicates higher confidence [28]. Moreover, the predicted domain structure of Phsocs5b is structurally similar to its mammalian counterparts [2,41].

Like all SOCS4-7 proteins (Fig. 1A), Phsocs5b harbored a long N-terminal region (1–405 aa), central SH2 domain (406–492 aa), and C-terminal SOCS box domain (508–544 aa) (Fig. 1B and C). SH2 and SOCS box domains are conserved and highly conserved domains, respectively, while the N-terminal region is a lowly conserved region [3]. The SH2 and SOCS box domains play important roles in determining the target of each SOCS family protein and recognizing the substrate for the poly-ubiquitination and subsequent degradation by the 26S proteasome, respectively [6,42].

Multiple sequence analysis of Phsocs5b illustrated a highly conserved amino acid sequence with other vertebrate orthologs (Fig. 2). The highest conservation was observed in the SH2 domain, and the

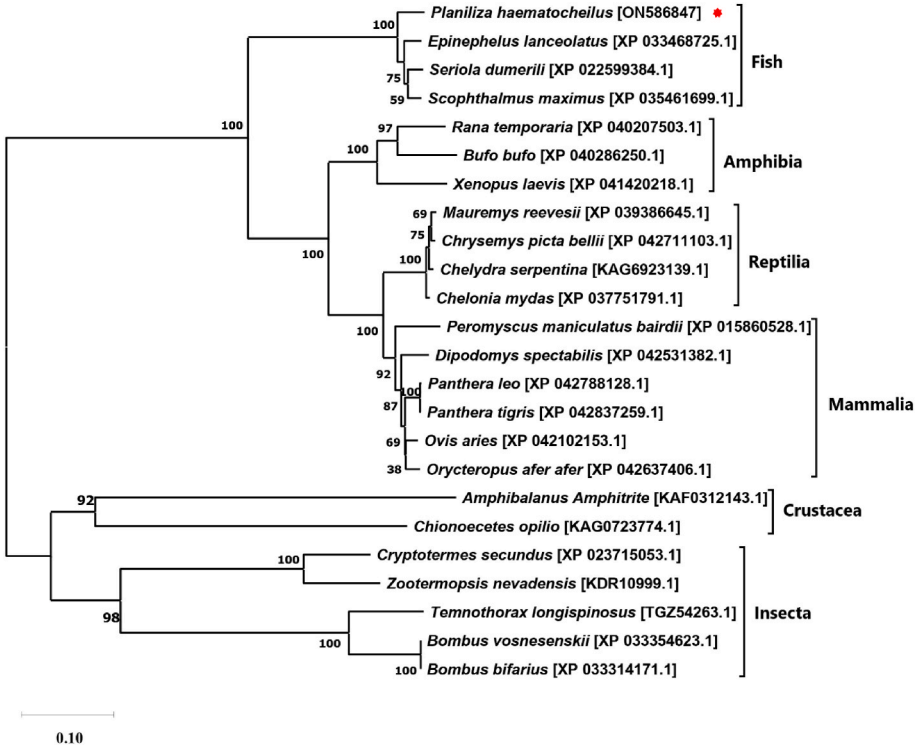

Fig. 3. Phylogenetic relationship of Phsocs5b with its other animal orthologs including Fish, Amphibia, Mammalia, Reptilia, Crustacea, and Insecta. Phsocs5b from *Planiliza haematocheilus* is clustered with the teleost clade. The phylogenetic tree was constructed using the neighbor-joining method, and bootstrap values are displayed on the branches based on 5000 replicates. NCBI accession numbers are shown next to the scientific name.

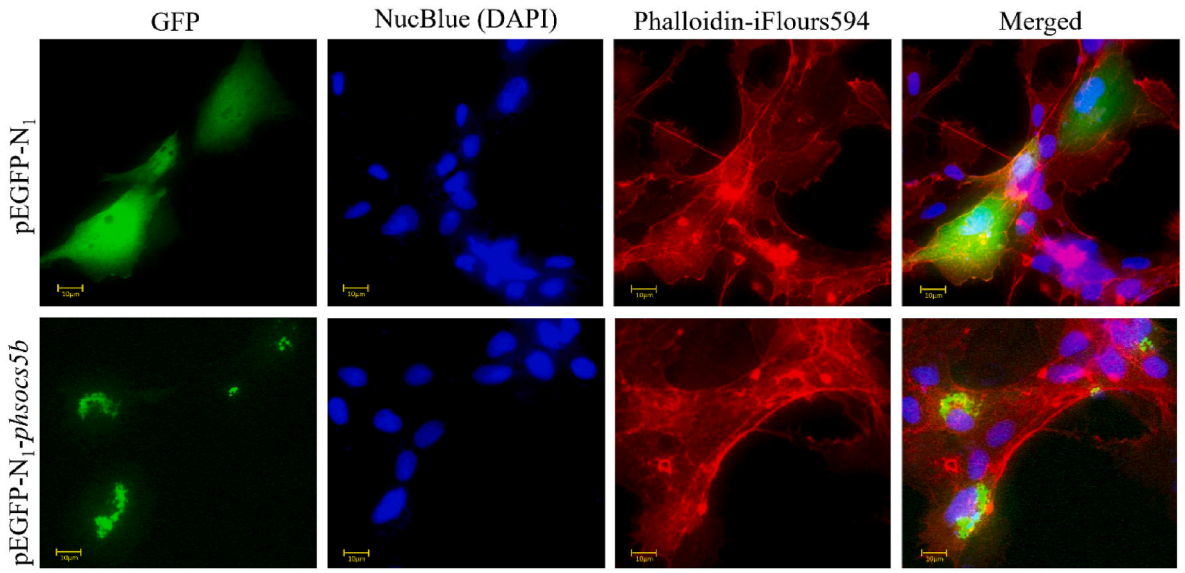

Fig. 4. Subcellular localization of Phsocs5b in FHM cells. FHM cells were transiently transfected with pEGFP-N1 **(A, B, C, and D)** or pEGFP-N1-*phsocs5b* **(E, F, G, and H)** and incubated at 25 °C for 24 h. Incubated cells were fixed using 4% formaldehyde. To visualize the cytoplasm, the nucleus and actin filaments were stained with NucBlue (DAPI) and Phalloidin-iFlours594. Images were captured using a fluorescence microscope. pEGFP-N1 or pEGFP-N1-*phsocs5b* expression is shown in green; the nucleus is indicated in blue; actin filaments in the cytoplasm are shown in red, and the merged results show the nucleus, cytoplasm, and fluorescence expression of pEGFP-N1 or pEGFP-N1-*phsocs5b* in the same cell.

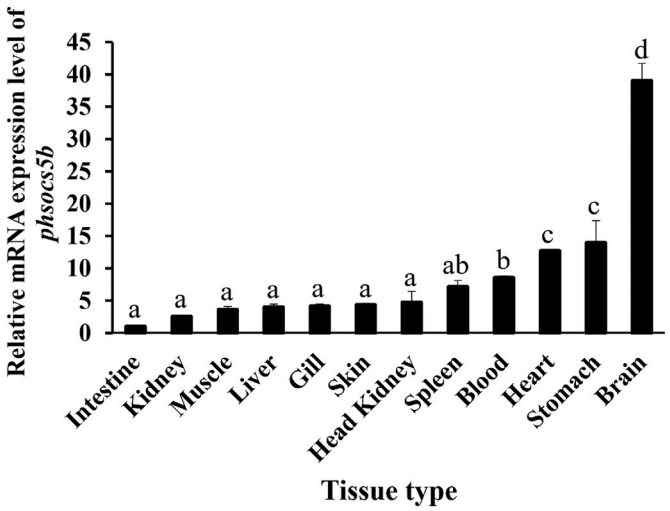

Fig. 5. Tissue-specific relative mRNA expression level of *phsocs5b* in healthy unchallenged redlip mullet. Relative mRNA expression levels in different organs are calculated relative to the mRNA expression level in the intestine. The expression of *phsocs5b* mRNA is the highest in the brain, while it is relatively higher in the stomach, heart, and blood than that in other tissues. Each bar represents the mean values of relative mRNA expression level ± standard deviation (SD) ($n = 3$). The statistical significance was determined using one-way ANOVA with Tukey's comparison. Different letters represent the statistically significant differences ($p < 0.05$) between the tissue types.

lowest conservation was in the N-terminal region. Pairwise sequence analysis with SOCS5 of fish, mammals, reptiles, and amphibians revealed that Phsocs5b has more than 60% and 70% of identity and similarity, respectively (Table 2). SOCS5 of *Epinephelus lanceolatus*, which belongs to fish taxonomy, showed the highest identity (95.0%) and similarity (96.8%) with the Phsocs5b. The lowest identity (62.3%) and similarity (73.5%) were observed with that of an amphibian (*Rana temporaria*). Consistent with our study, Ye et al. showed that SOCS family proteins of yellow catfish (*Pelteobagrus fulvidraco*) shared a conserved SOCS domain and SH2 domain with mammals, amphibians, and fish [19]. Furthermore, they revealed that SOCS5 of yellow catfish has more than 77% identity with the SOCS5 orthologs of *Ictalurus punctatus*, *Danio rerio*, *Xiphophorus maculatus*, *Mus musculus,* and *Homo sapiens* [19]. Nevertheless, phylogenetic tree construction illustrated that Phsocs5b clustered with the teleost clade with a 100% bootstrap value (Fig. 3).

3.2. *Phsocs5b is localized in the cytoplasm of FHM cells*

Fluorescence imaging analysis of FHM cells after the transfection of GFP-tagged pEGFP-N1 plasmid and pEGFP-N1-*phsocs5b* construct revealed that Phsocs5b was localized in the cytoplasm and mostly around the nucleus (Fig. 4). Previous studies also unveiled that mammalian SOCS1 [43] and SOCS3 [44] localized in the cytoplasm and around the nucleus, respectively. Nevertheless, Kario et al. stated that mammalian SOCS5 co-localizes with the EGFR in intracellular vesicles in the cytoplasm [16].

3.3. *Tissue distribution of phsocs5b in redlip mullet*

The mRNA expression level of *phsocs5b* in different tissues of redlip mullet was analyzed using RT-qPCR (Fig. 5). The highest *phsocs5b* mRNA expression level was observed in the brain (~38.2 fold), followed by those in the stomach (~14.3 fold), heart (~12.8 fold), and blood (~8.2 fold). However, *phsocs5b* mRNA expression levels in other tissues showed relatively lower expression levels, and the intestine had the lowest. Consistent with our result, Brender et al. also stated that mammalian SOCS5 is expressed in many tissues, while a high expression level of SOCS5 was observed in the brain of the BALB/c mice [4].

3.4. *Immune stimulants enhance phsocs5b expression in blood extracted from redlip mullet in vivo*

Innate immunity is the first line of defense against pathogen infections and wounds in animals. The innate immune response is a quick action and the immune cells are able to recognize specific molecules found on different pathogens [45]. Blood plays an important role in innate immunity as a barrier against foreign invaders, such as microbial and parasitic infections, and regulates inflammation and

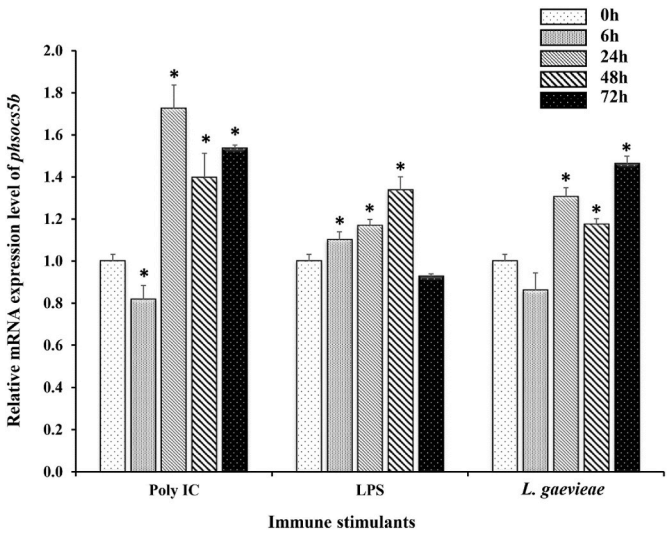

Fig. 6. Relative mRNA expression level of *phsocs5b* in the blood of redlip mullet after 0, 6, 24, 48, and 72 h following Poly I:C, LPS, and *L. gaevieae* challenges. RT-qPCR analysis of the blood was done to investigate the changes in *PhSOCS5b* transcription level after the immune challenges. The fold expression values were normalized to that of the untreated control (at 0 h). Data are shown as mean relative mRNA expression level ± SD ($n = 3$). *Statistical significance ($p < 0.05$) of the differences between the control and each experimental group was calculated using Student's *t*-test.

damage-induced signals [46]. Furthermore, blood is a medium for several immune cells, including neutrophils and macrophages, which are essential in innate immunity as immune sentinel cells to attack pathogens and repair damage at first sight [47,48]. Moreover, these immune cells quickly interact with pathogens to kill them and help to activate the cells related to adaptive immunity [45]. This fast response of blood cells may be beneficial to analyze the temporal changes in the expression of immune-related genes against pathogen infections.

Therefore, we investigated the temporal changes in *phsocs5b* mRNA expression in redlip mullet blood following immune stimulation with Poly I:C, LPS, and *L. gaevieae* at different time points (Fig. 6). Poly I:C is a double-stranded RNA virus mimic, LPS is a lipopolysaccharide extracted from *E. coli,* and *L. garvieae* is a gram-positive bacterial pathogen that mostly affects saltwater fish. As expected, all three stimulants potentiated the *phsocs5b* mRNA expression in blood in a time-dependent manner. However, Poly I:C and *L. garvieae* showed undulatory modulation of *phsocs5b* mRNA level: at 6 h p.i.; Poly I:C and *L. garvieae* reduced the *phsocs5b* mRNA expression, wherein the highest level of *phsocs5b* mRNA expression was observed at 24 h p.i. with Poly I:C. LPS stimulated the expression in a time-dependent manner until 48 h, and at 72 h, a reduced *phsocs5b* mRNA expression was observed. The undulatory modulation pattern observed in the current study could be attributed to the complex mechanisms of several immune-related signaling pathways in cells. This complexity occurs due to a large number of components and isoforms that have partially overlapping functions [49]. Each pathway has a specific temporal activation pattern against pathogen invasion [50], and several pathways may control each molecule. Nevertheless, these results revealed that Phsocs5b hinders the virus or bacterial infection as an immune response.

3.5. Phsocs5b impairs VHSV infection in vitro

In vivo immune challenge experimental results prompted us to investigate the regulatory effect of Phsocs5b against VHSV infection as a stimulant. For this purpose, FHM cells ectopically expressing Phsocs5b were infected with GFP-tagged VHSV, and fluorescence images were captured at 12 and 24 h p.i. Furthermore, VHSV copy numbers at different time points (0, 12, 24, and 48 h p.i.), relative mRNA expression levels of the genes encoding virus G-, P-, N-, and R-proteins at 24 h p.i., and the virus titer in the supernatant (cell culture medium) at 12 and 24 h p.i. were analyzed (Fig. 7).

SOCS family proteins are commonly identified as negative regulators of cytokine signaling [2,5,6,9,10,13]. Therefore, SOCS family proteins may potentiate virus invasion and replication [2]. Paradoxically, our findings revealed attenuated VHSV infection and replication upon Phsocs5b overexpression in FHM cells compared to the control (Fig. 7). As shown in Fig. 7A, GFP expression in Phsocs5b-overexpressing FHM

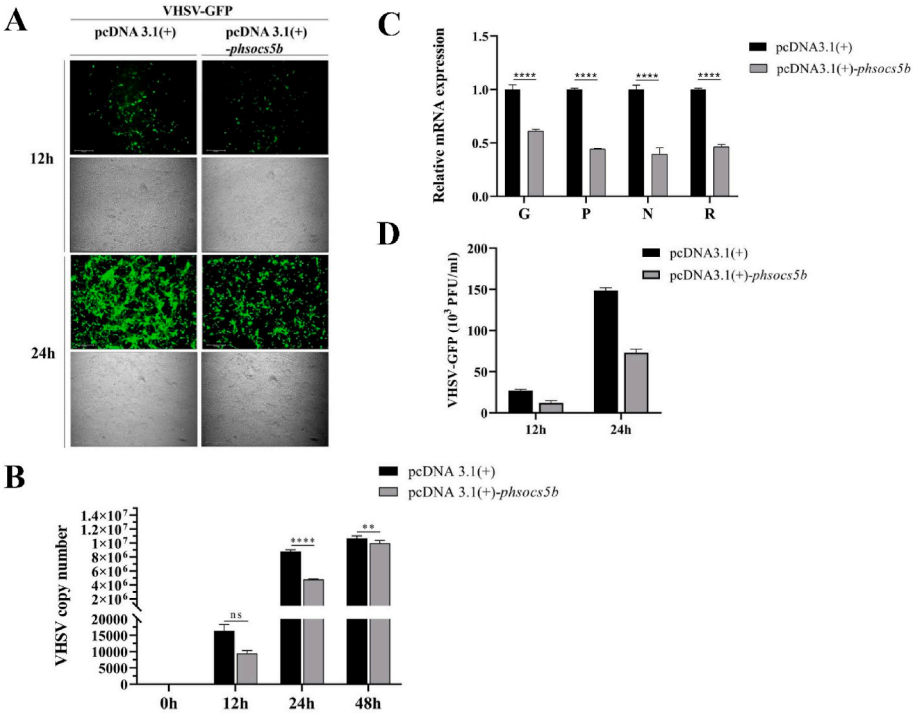

Fig. 7. Phsocs5b negatively regulates anti-viral replication. GFP fluorescence expression **(A)** viral hemorrhagic septicemia virus (VHSV) copy number **(B)** and relative mRNA expression levels of genes encoding virus G-, P-, N-, and R-proteins **(C),** Viral titer in the supernatant **(D)** were measured in pcDNA3.1(+)(control) or pcDNA3.1 (+)-*phsocs5b* transiently transfected FHM cells after rVHSV-ΔNV-GFP (0.01 MOI) infection. All the data are represented as the mean values ± SD ($n = 3$). Statistical significances between PhSOCS5b-overexpressing and control cells were analyzed using Student's *t*-test (ns; $p > 0.05$; **, $p \leq 0.01$; ****, $p \leq 0.0001$).

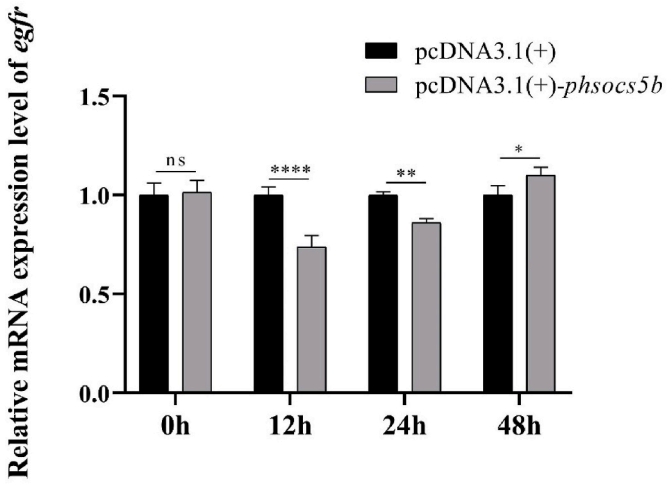

Fig. 8. Phsocs5b negatively regulates *egfr*. FHM cells were transiently transfected with pcDNA3.1(+) or pcDNA3.1 (+)-*phsocs5b*. After 0, 12, 24, and 48 h, the expression level of *egfr* was analyzed using RT-qPCR. Values are shown as mean ± SD ($n = 3$). Student's *t*-test was performed to analyze the statistical significance of the differences between the control and Phsocs5b overexpressing cells. Statistical significance is indicated using asterisks (ns, $p > 0.05$; *, $p \leq 0.05$; **, $p \leq 0.01$; ****, $p \leq 0.0001$).

cells was reduced at 12 and 24 h p.i. upon VHSV infection compared to that in control cells. VHSV copy number was significantly reduced in FHM cells overexpressing Phsocs5b at 12, 24, and 48 h p.i., compared to that in control, while the highest difference was observed at 24 h p.i. (Fig. 7B). Phsocs5b overexpression significantly reduced the mRNA level of genes encoding viral G-, P-, N-, and R-proteins at 24 h p.i. (Fig. 7C). Moreover, plaque assay results also confirmed low amounts of viral titer in the culture medium of Phsocs5b-overexpressing cells than those in the control (Fig. 7D). Taken together, these results imply that Phsocs5b negatively regulates VHSV infections.

3.6. Phsocs5b negatively regulates egfr transcription

EGFR is a transmembrane protein that belongs to the receptor tyrosine kinase family and is extensively expressed in a variety of cell types, such as epithelial and mesenchymal cells [51]. Several studies have demonstrated that EGFR facilitates the cell entry of many viruses, including hepatitis C virus, herpes simplex virus 1, human cytomegalovirus, transmissible gastroenteritis virus, and IAV via different mechanisms [52–55]. Therefore, in the present study, we analyzed the expression level of *egfr* at 0, 12, 24, and 48 h p.i. in Phsocs5b-overexpressing cells using RT-qPCR to assess the effect of Phsocs5b on Egfr. Here we demonstrated that Phsocs5b overexpression significantly reduced *egfr* transcription at 12 and 24 h p.i. (Fig. 8). Concordant with our study, Kario et al. have reported that SOCS proteins use the SH2 domain to recognize the substrate; subsequently, the SOCS box domain interacts with the EGFR and promotes its degradation [16]. As SOCS5 is directly involved in the degradation of the EGFR protein, the effect of Phsocs5b on the attenuation of *egfr* transcription remains unclear. Therefore, although the reduced *egfr* expression obtained in this study supports the effects of attenuation of VHSV infections, further studies are required to investigate whether EGFR facilitates the cell entry of VHSV and understand its mechanism.

3.7. Phsocs5b induces Pi3k/Akt pathway and enhances cell proliferation and migration

EGFR activates the PI3K/AKT signaling pathway, which is indispensable for cytoskeleton reorganization, cellular protein synthesis, transcriptional activation, apoptotic inhibition, and cell proliferation

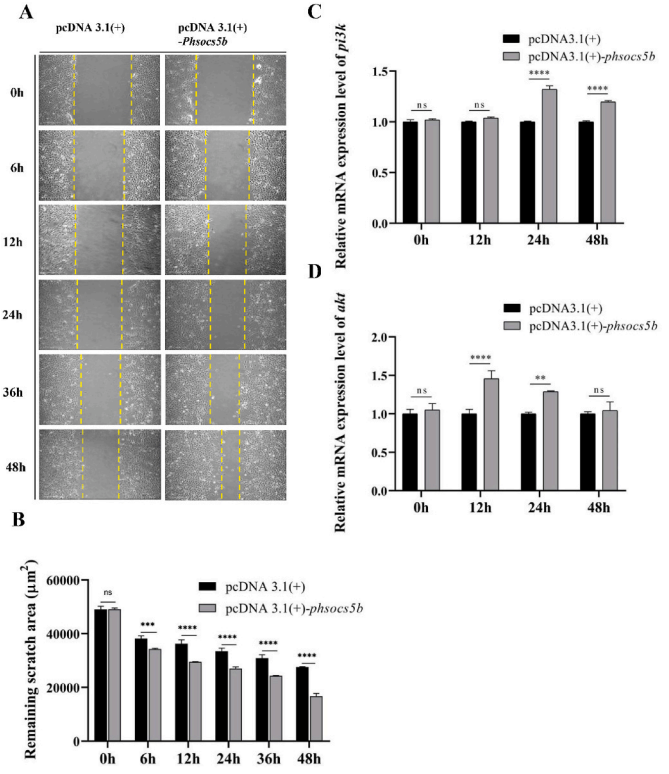

Fig. 9. Phsocs5b enhances *pi3k* and *akt* expression and increases cell migration and proliferation. Scratch assay comparing the effect of Phsocs5b on cell migration compared to the control (empty vector) **(A)**. FHM cells were transiently transfected with pcDNA3.1(+)(control) or pcDNA3.1 (+)-*phsocs5b*; at 24 h post-transfection, a scratch was made across the well bottom of the cell culture plate, and images were taken at 0, 6, 12, 24, 36, and 48 h time points. The remaining scratch areas **(B)** were calculated using Digimizer Version 5.4.4 software at each time point. Relative mRNA expression levels of *pi3k* **(C)** and *akt* **(D)** were analyzed using RT-qPCR after transient transfection of pcDNA3.1 (+)(control) or pcDNA3.1 (+)-*phsocs5b* in FHM cells. All the data are represented as mean ± SD ($n = 3$), and statistical significance levels were calculated using the Student's *t*-test (ns, $p > 0.05$; **, $p \leq 0.01$; ***, $p \leq 0.001$; ****, $p \leq 0.0001$).

and survival [18,55]. Therefore, we conducted a scratch assay to determine whether Phsocs5b negatively regulates cell proliferation. The results demonstrated that Phsocs5b reduced the scratch area in Phsocs5b-overexpressing cells compared to that in the control cells (Fig. 9A and B), suggesting that Phsocs5b potentiates cell proliferation and migration.

Next, we analyzed the transcription level of *pi3k* and *akt* using RT-qPCR at different time points (0, 12, 24, and 48 h) post-transfection (Fig. 9C and D). The results revealed that Phsocs5b significantly enhanced the transcriptional level of *pi3k* at 24 and 48 h (Fig. 9C). Furthermore, a significant increase in *akt* transcription level was observed at 12 and 24 h (Fig. 9D) in Phsocs5b-overexpressing cells compared to that in control cells. Consistent with our observation, a previous study has shown that SOCS5 directly induces the PI3K/AKT pathway and facilitates cell migration and invasion via autophagy inhibition by targeting PI3K [56]. These results suggest that Phsocs5b itself induces the Pi3k/Akt pathway and enhances cell proliferation and migration. Furthermore, we speculated that the activation of the Pi3k/Akt signaling pathway could have enhanced the feedback mechanism to suppress *egfr* mRNA expression (Fig. 8).

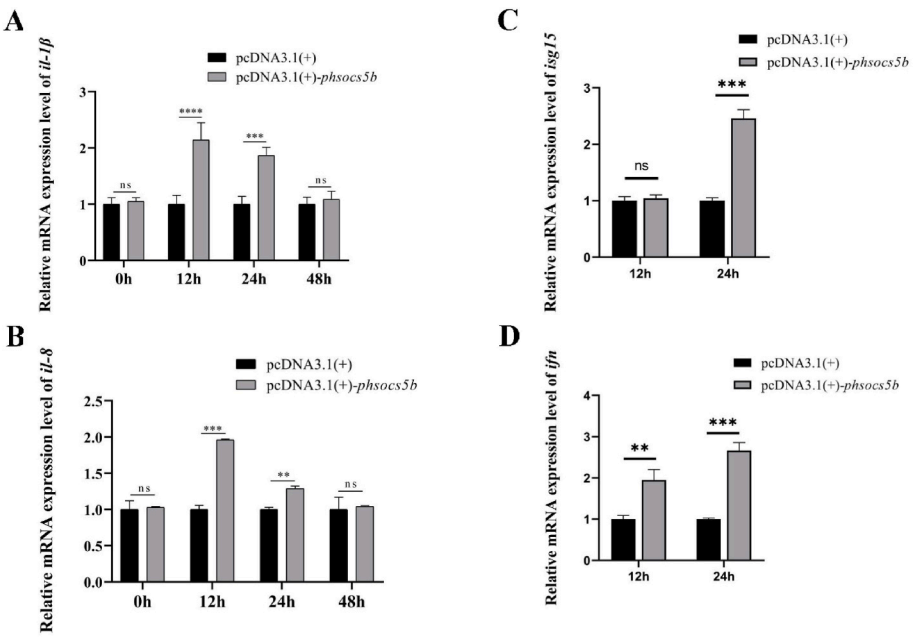

Fig. 10. Phsocs5b overexpression induces pro-inflammatory cytokine secretion and anti-viral gene expression. Relative mRNA expression levels of pro-inflammatory cytokines (*il1β* **(A)**, *il8* **(B)**) and anti-viral genes (*isg15* **(C)** and *ifn* **(D)**) in pcDNA3.1(+) (control) or pcDNA3.1 (+)-*phsocs5b*-transfected FHM cells upon VHSV infection. Data are shown as mean ± SD ($n = 3$). The statistical significance of differences in relative mRNA expression of pro-inflammatory cytokines between the control and PhSOCS5b-overexpressing FHM cells were calculated using the Student's *t*-test (ns, $p > 0.05$; **, $p \leq 0.01$; ***, $p \leq 0.001$; ****, $p \leq 0.0001$).

3.8. Phsocs5b positively regulates cytokine and anti-viral gene transcription

The effect of Phsocs5b on cytokine secretion and anti-viral gene expression was investigated by overexpressing Phsocs5b in FHM cells followed by VHSV infection. The results showed that the expression of pro-inflammatory cytokines (*il1β* and *il8;* Fig. 10A and B) and anti-viral genes (*isg15* and *ifn;* Fig. 10C and D) were significantly induced at 12 and 24 h p.i. The expression level of both cytokines was more pronounced at 12 h p.i. and the anti-viral genes were highly expressed at 24 h p.i. A previous study has demonstrated that inhibition of PI3K by Wortmannin and LY294002 reduces the production of IL-1β, IL-6, IL-8, TNF-α, and IFN-γ [57]. Tian et al. also reported that blocking the PI3K/AKT pathway suppressed IFN-stimulated genes in mammals [58]. Numerous studies have reported that PI3K/AKT pathway is also involved in Toll-like receptor signaling and cytokine secretion induction [59,60]. Taken together, our results suggest that overexpression of Phsocs5b enhances the activation of Pi3k, thus inducing the production of pro-inflammatory cytokines (Il-1β and Il-8) and anti-viral proteins (Isg15 and Ifn).

4. Conclusion

In this study, we identified that Phsocs5b, highly expressed in the brain of redlip mullet, is identical to known orthologs identified in other vertebrates. It comprises a highly conserved SH2 domain, SOCS box domain, and less conserved long N-terminal region. Phsocs5b improved the innate immunity upon Poly I:C, LPS, and *L. gaevieae* challenges *in vivo*. In FHM cells, overexpression of Phsocs5b attenuated VHSV invasion and replication via degradation of Egfr. On the contrary, it activated the Pi3k/Akt pathway, which enhanced cell proliferation and migration. Phsocs5b promoted the Il-1β and Il-8 pro-inflammatory cytokine secretion and *Isg15* and *Ifn* anti-viral gene expression. These findings suggest that Phsocs5b attenuates virus infections through the degradation of Egfr and enhances the production of pro-inflammatory cytokines and anti-viral proteins while enhancing cell proliferation and migration by activating Pi3k/Akt pathway. Therefore, Phsocs5b may be a potential target to enhance the innate immune response and cell proliferation. However, further studies are required to understand the exact mechanism of Phsocs5b in immune regulation.

CRediT authorship contribution statement

H.M.S.M. Wijerathna: Conceptualization, Methodology, Investigation, Formal analysis, Writing – original draft. **Kishanthini Nadarajapillai:** Methodology, Investigation, Writing – review & editing. **K.A. S.N. Shanaka:** Methodology, Investigation, Writing – review & editing. **T.D.W. Kasthuriarachchi:** Methodology, Investigation. **Sumi Jung:** Methodology, Investigation. **Seongdo Lee:** Methodology, Investigation. **Jehee Lee:** Resources, Supervision, Writing – review & editing, Project administration, Funding acquisition.

Data availability

Data will be made available on request.

Acknowledgments

This research was supported by the Basic Science Research Program through the National Research Foundation of Korea (NRF), funded by the Ministry of Education (2019R1A6A1A03033553), and Korea Institute of Marine Science & Technology Promotion (KIMST), funded by the Ministry of Oceans and Fisheries (20220570).

References

[1] H.-J. Jin, J.-Z. Shao, L.-X. Xiang, H. Wang, L.-L. Sun, Global identification and comparative analysis of SOCS genes in fish: insights into the molecular evolution of SOCS family, Mol. Immunol. 45 (2008) 1258–1268, https://doi.org/10.1016/j.molimm.2007.09.015.

[2] L. Larsen, C. Ropke, Suppressors of cytokine signaling: SOCS. Review article, APMIS 110 (2002) 833–844, https://doi.org/10.1034/j.1600-0463.2002.1101201.x.

[3] D. Zhou, L. Chen, K. Yang, H. Jiang, W. Xu, J. Luan, SOCS molecules: the growing players in macrophage polarization and function, Oncotarget 8 (2017) 60710–60722, https://doi.org/10.18632/oncotarget.19940.

[4] C. Brender, R. Columbus, D. Metcalf, E. Handman, R. Starr, N. Huntington, D. Tarlinton, N. Ødum, S.E. Nicholson, N.A. Nicola, D.J. Hilton, W.S. Alexander, SOCS5 is expressed in primary B and T lymphoid cells but is dispensable for lymphocyte production and function, Mol. Cell Biol. 24 (2004) 6094–6103, https://doi.org/10.1128/MCB.24.13.6094-6103.2004.

[5] A. Sasaki, H. Yasukawa, A. Suzuki, S. Kamizono, T. Syoda, I. Kinjyo, M. Sasaki, J. A. Johnston, A. Yoshimura, Cytokine-inducible SH2 protein-3 (CIS3/SOCS3) inhibits Janus tyrosine kinase by binding through the N-terminal kinase inhibitory region as well as SH2 domain: molecular mechanism of JAK2 inhibition by CIS3, Gene Cell. 4 (1999) 339–351, https://doi.org/10.1046/j.1365-2443.1999.00263.x.

[6] A. Yoshimura, H. Yasukawa, JAK's SOCS: a mechanism of inhibition, Immunity 36 (2012) 157–159, https://doi.org/10.1016/j.immuni.2012.01.010.

[7] H.-M. Zhao, R. Xu, X.-Y. Huang, S.-M. Cheng, M.-F. Huang, H.-Y. Yue, X. Wang, Y. Zou, A.-P. Lu, D.-Y. Liu, Curcumin suppressed activation of dendritic cells via JAK/STAT/SOCS signal in mice with experimental colitis, Front. Pharmacol. 7 (2016), https://doi.org/10.3389/fphar.2016.00455.

[8] M. Maruoka, S. Kedashiro, Y. Ueda, K. Mizutani, Y. Takai, Nectin-4 co-stimulates the prolactin receptor by interacting with SOCS1 and inhibiting its activity on the JAK2-STAT5a signaling pathway, J. Biol. Chem. 292 (2017) 6895–6909, https://doi.org/10.1074/jbc.M116.769091.

[9] A. Matsumoto, M. Masuhara, K. Mitsui, M. Yokouchi, M. Ohtsubo, H. Misawa, A. Miyajima, A. Yoshimura, CIS, a cytokine inducible SH2 protein, is a target of the JAK-STAT5 pathway and modulates STAT5 activation, Blood 89 (1997) 3148–3154, https://doi.org/10.1182/blood.V89.9.3148.

[10] N.P.D. Liau, A. Laktyushin, I.S. Lucet, J.M. Murphy, S. Yao, E. Whitlock, K. Callaghan, N.A. Nicola, N.J. Kershaw, J.J. Babon, The molecular basis of JAK/STAT inhibition by SOCS1, Nat. Commun. 9 (2018) 1558, https://doi.org/10.1038/s41467-018-04013-1.

[11] G.M. Tannahill, J. Elliott, A.C. Barry, L. Hibbert, N.A. Cacalano, J.A. Johnston, SOCS2 can enhance interleukin-2 (IL-2) and IL-3 signaling by accelerating SOCS3 degradation, Mol. Cell Biol. 25 (2005) 9115–9126, https://doi.org/10.1128/MCB.25.20.9115-9126.2005.

[12] S. Haan, SOCS2 physiological and pathological functions, Front. Biosci. 8 (2016) 189–204, https://doi.org/10.2741/e760.

[13] Y. Seki, K. Hayashi, A. Matsumoto, N. Seki, J. Tsukada, J. Ransom, T. Naka, T. Kishimoto, A. Yoshimura, M. Kubo, Expression of the suppressor of cytokine signaling-5 (SOCS5) negatively regulates IL-4-dependent STAT6 activation and Th2 differentiation, Proc. Natl. Acad. Sci. USA 99 (2002) 13003–13008, https://doi.org/10.1073/pnas.202477099.

[14] A. Sanchez-Mejias, J. Kwon, X.H. Chew, A. Siemens, H.S. Sohn, G. Jing, B. Zhang, H. Yang, Y. Tay, A novel SOCS5/miR-18/miR-25 axis promotes tumorigenesis in liver cancer: SOCS5/miR-18/miR-25 axis promotes tumorigenesis, Int. J. Cancer 144 (2019) 311–321, https://doi.org/10.1002/ijc.31857.

[15] Y. Fu, Y. Xu, S. Chen, Y. Ouyang, G. Sun, MiR-151a-3p promotes postmenopausal osteoporosis by targeting SOCS5 and activating JAK2/STAT3 signaling, Rejuvenation Res. 23 (2020) 313–323, https://doi.org/10.1089/rej.2019.2239.

[16] E. Kario, M.D. Marmor, K. Adamsky, A. Citri, I. Amit, N. Amariglio, G. Rechavi, Y. Yarden, Suppressors of cytokine signaling 4 and 5 regulate epidermal growth factor receptor signaling, J. Biol. Chem. 280 (2005) 7038–7048, https://doi.org/10.1074/jbc.M408575200.

[17] L. Kedzierski, M.D. Tate, A.C. Hsu, T.B. Kolesnik, E.M. Linossi, L. Dagley, Z. Dong, S. Freeman, G. Infusini, M.R. Starkey, N.L. Bird, S.M. Chatfield, J.J. Babon, N. Huntington, G. Belz, A. Webb, P.A. Wark, N.A. Nicola, J. Xu, K. Kedzierska, P. M. Hansbro, S.E. Nicholson, Suppressor of cytokine signaling (SOCS)5 ameliorates influenza infection via inhibition of EGFR signaling, Elife 6 (2017), e20444, https://doi.org/10.7554/eLife.20444.

[18] N. Prenzel, O.M. Fischer, S. Streit, S. Hart, A. Ullrich, The epidermal growth factor receptor family as a central element for cellular signal transduction and diversification, Endocr. Relat. Cancer (2001) 11–31, https://doi.org/10.1677/erc.0.0080011.

[19] H.-M. Ye, T. Zhao, L.-X. Wu, J. Cheng, X.-Y. Tan, Molecular characterization of nine suppressors of cytokine signaling (SOCS) genes from yellow catfish *Pelteobagrus fulvidraco* and their changes in mRNA expression to dietary carbohydrate levels, Fish Shellfish Immunol. 86 (2019) 906–912, https://doi.org/10.1016/j.fsi.2018.12.037.

[20] Hyun-Ja Han, Nam Sil Lee, Myoung Sug Kim, Sung-Hee Jung, An outbreak of Lactococcus garvieae infection in cage-cultured red lip mullet *Chelon haematocheilus* with green liver syndrome, Fish. Aquat. Sci. 18 (2015) 333–339, https://doi.org/10.5657/FAS.2015.0333.

[21] Ministry of Oceans and Fisehries, The Current Fish Culture by City & Province, Ward & County, by Culture Type by Species, Ministry of Oceans and Fisehries, 2022. https://kosis.kr/statHtml/statHtml.do?orgId=101&tblId=DT_1EZ0008&conn_path=I2&language=en. (Accessed 2 August 2022).

[22] W.-S. Kim, J.-H. Kim, M.-S. Jang, S.-J. Jung, M.-J. Oh, Infection of wild mullet (*Mugil cephalus*) with Myxobolus episquamalis in Korea, Parasitol. Res. 112 (2013) 447–451, https://doi.org/10.1007/s00436-012-3075-7.

[23] Sung-Woo Park, Jin-Ha Yu, Chun-Hee Lee, Amyloodinium sp. Infestation in Mullet (*Mugil cephalus*) cultured in a pond on land, J. Fish Pathol. 19 (2006) 7–15.

[24] S. McGinnis, T.L. Madden, BLAST: at the core of a powerful and diverse set of sequence analysis tools, Nucleic Acids Res. 32 (2004) W20–W25, https://doi.org/10.1093/nar/gkh435.

[25] K. Okonechnikov, O. Golosova, M. Fursov, Unipro UGENE: a unified bioinformatics toolkit, Bioinformatics 28 (2012) 1166–1167, https://doi.org/10.1093/bioinformatics/bts091.

[26] J. Schultz, F. Milpetz, P. Bork, C.P. Ponting, SMART, a simple modular architecture research tool: identification of signaling domains, Proc. Natl. Acad. Sci. USA 95 (1998) 5857–5864, https://doi.org/10.1073/pnas.95.11.5857.

[27] A. Marchler-Bauer, M.K. Derbyshire, N.R. Gonzales, S. Lu, F. Chitsaz, L.Y. Geer, R. C. Geer, J. He, M. Gwadz, D.I. Hurwitz, C.J. Lanczycki, F. Lu, G.H. Marchler, J. S. Song, N. Thanki, Z. Wang, R.A. Yamashita, D. Zhang, C. Zheng, S.H. Bryant, CDD: NCBI's conserved domain database, Nucleic Acids Res. 43 (2015) D222–D226, https://doi.org/10.1093/nar/gku1221.

[28] Y. Zhang, I-TASSER server for protein 3D structure prediction, BMC Bioinf. 9 (2008) 40, https://doi.org/10.1186/1471-2105-9-40.

[29] W.L. DeLano, PyMOL: an open-source molecular graphics tool, CCP4 Newsl Protein Crystallogr 40 (2002) 82–92.

[30] F. Sievers, D.G. Higgins, in: K. Katoh (Ed.), The Clustal Omega Multiple Alignment Package, Mult. Seq. Alignment, Springer US, New York, NY, 2021, pp. 3–16, https://doi.org/10.1007/978-1-0716-1036-7_1.

[31] P. Rice, I. Longden, A. Bleasby, EMBOSS: the European molecular biology open software suite, Trends Genet. 16 (2000) 276–277, https://doi.org/10.1016/S0168-9525(00)02024-2.

[32] K. Tamura, G. Stecher, S. Kumar, MEGA11: molecular evolutionary genetics analysis version 11, Mol. Biol. Evol. 38 (2021) 3022–3027, https://doi.org/10.1093/molbev/msab120.

[33] R. Johansen, J.R. Needham, D.J. Colquhoun, T.T. Poppe, A.J. Smith, Guidelines for health and welfare monitoring of fish used in research, Lab. Anim. 40 (2006) 323–340.

[34] M. Oh, N. Umasuthan, D.A.S. Elvitigala, Q. Wan, E. Jo, J. Ko, G.E. Noh, S. Shin, S. Rho, J. Lee, First comparative characterization of three distinct ferritin subunits from a teleost: evidence for immune-responsive mRNA expression and iron depriving activity of seahorse (*Hippocampus abdominalis*) ferritins, Fish Shellfish Immunol. 49 (2016) 450–460, https://doi.org/10.1016/j.fsi.2015.12.039.

[35] R. Owczarzy, A.V. Tataurov, Y. Wu, J.A. Manthey, K.A. McQuisten, H. G. Almabrazi, K.F. Pedersen, Y. Lin, J. Garretson, N.O. McEntaggart, C.A. Sailor, R. B. Dawson, A.S. Peek, IDT SciTools: a suite for analysis and design of nucleic acid oligomers, Nucleic Acids Res. 36 (2008) W163, https://doi.org/10.1093/nar/gkn198. –W169.

[36] K.J. Livak, T.D. Schmittgen, Analysis of relative gene expression data using real-time quantitative PCR and the $2^{-\Delta\Delta CT}$ method, Methods 25 (2001) 402–408, https://doi.org/10.1006/meth.2001.1262.

[37] M. Kim, D. Kim, K. Kim, Generation and characterization of NV gene-knockout recombinant viral hemorrhagic septicemia virus (VHSV) genotype IVa, Dis. Aquat. Org. 97 (2011) 25–35, https://doi.org/10.3354/dao02394.

[38] J.-O. Kim, W.-S. Kim, S.-W. Kim, H.-J. Han, J. Kim, M. Park, M.-J. Oh, Development and application of quantitative detection method for viral hemorrhagic septicemia virus (VHSV) genogroup IVa, Viruses 6 (2014) 2204–2213, https://doi.org/10.3390/v6052204.

[39] K. Chathuranga, T. Kim, H. Lee, J. Park, J. Kim, W.A.G. Chathuranga, P. Ekanayaka, Y.J. Choi, C. Lee, C. Kim, J.U. Jung, J. Lee, Negative regulation of NEMO signaling by the ubiquitin E3 ligase MARCH2, EMBO J. 39 (2020), https://doi.org/10.15252/embj.2020105139.

[40] P.G. Righetti, Determination of the isoelectric point of proteins by capillary isoelectric focusing, J. Chromatogr. A 1037 (2004) 491–499, https://doi.org/10.1016/j.chroma.2003.11.025.

[41] M. Fujimoto, T. Naka, SOCS1, a negative regulator of cytokine signals and TLR responses, in human liver diseases, 2010, Gastroenterol. Res. Pract. (2010) 1–7, https://doi.org/10.1155/2010/470468.

[42] E.M. Linossi, S.E. Nicholson, The SOCS box-adapting proteins for ubiquitination and proteasomal degradation, IUBMB Life 64 (2012) 316–323, https://doi.org/10.1002/iub.1011.

[43] B.Q. Vuong, T.L. Arenzana, B.M. Showalter, J. Losman, X.P. Chen, J. Mostecki, A. S. Banks, A. Limnander, N. Fernandez, P.B. Rothman, SOCS-1 localizes to the microtubule organizing complex-associated 20S proteasome, Mol. Cell Biol. 24 (2004) 9092–9101, https://doi.org/10.1128/MCB.24.20.9092-9101.2004.

[44] J. Xie, M. Wang, A. Cheng, X.-X. Zhao, M. Liu, D. Zhu, S. Chen, R. Jia, Q. Yang, Y. Wu, S. Zhang, Y. Liu, Y. Yu, L. Zhang, X. Chen, DHAV-1 inhibits type I interferon signaling to assist viral adaption by increasing the expression of SOCS3, Front. Immunol. 10 (2019) 731, https://doi.org/10.3389/fimmu.2019.00731.

[45] A.E. Thompson, The immune System, JAMA 313 (2015) 1686, https://doi.org/10.1001/jama.2015.2940.

[46] I. Vlisidou, W. Wood, Drosophila blood cells and their role in immune responses, FEBS J. 282 (2015) 1368–1382, https://doi.org/10.1111/febs.13235.

[47] B. Alberts (Ed.), Molecular Biology of the Cell, fourth ed., Garland Science, New York, 2002.

[48] Y. Su, J. Gao, P. Kaur, Z. Wang, Neutrophils and macrophages as targets for development of nanotherapeutics in inflammatory diseases, Pharmaceutics 12 (2020) 1222, https://doi.org/10.3390/pharmaceutics12121222.

[49] G. Weng, U.S. Bhalla, R. Iyengar, Complexity in biological signaling systems, Science 284 (1999) 92–96, https://doi.org/10.1126/science.284.5411.92.

[50] M. Boutros, H. Agaisse, N. Perrimon, Sequential activation of signaling pathways during innate immune responses in Drosophila, Dev. Cell 3 (2002) 711–722, https://doi.org/10.1016/S1534-5807(02)00325-8.

[51] A. Wells, EGF receptor, Int. J. Biochem. Cell Biol. 31 (1999) 637–643, https://doi.org/10.1016/S1357-2725(99)00015-1.

[52] G. Chan, M.T. Nogalski, A.D. Yurochko, Activation of EGFR on monocytes is required for human cytomegalovirus entry and mediates cellular motility, Proc. Natl. Acad. Sci. USA 106 (2009) 22369–22374, https://doi.org/10.1073/pnas.0908787106.

[53] T. Eierhoff, E.R. Hrincius, U. Rescher, S. Ludwig, C. Ehrhardt, The epidermal growth factor receptor (egfr) promotes uptake of influenza A viruses (IAV) into host cells, PLoS Pathog. 6 (2010), e1001099, https://doi.org/10.1371/journal.ppat.1001099.

[54] J. Lupberger, M.B. Zeisel, F. Xiao, C. Thumann, I. Fofana, L. Zona, C. Davis, C. J. Mee, M. Turek, S. Gorke, C. Royer, B. Fischer, M.N. Zahid, D. Lavillette, J. Fresquet, F.-L. Cosset, S.M. Rothenberg, T. Pietschmann, A.H. Patel, P. Pessaux, M. Doffoël, W. Raffelsberger, O. Poch, J.A. McKeating, L. Brino, T.F. Baumert, EGFR and EphA2 are host factors for hepatitis C virus entry and possible targets for antiviral therapy, Nat. Med. 17 (2011) 589–595, https://doi.org/10.1038/nm.2341.

[55] W. Hu, S. Zhang, Y. Shen, Q. Yang, Epidermal growth factor receptor is a co-factor for transmissible gastroenteritis virus entry, Virology 521 (2018) 33–43, https://doi.org/10.1016/j.virol.2018.05.009.
[56] M. Zhang, S. Liu, M.-S. Chua, H. Li, D. Luo, S. Wang, S. Zhang, B. Han, C. Sun, SOCS5 inhibition induces autophagy to impair metastasis in hepatocellular carcinoma cells via the PI3K/Akt/mTOR pathway, Cell Death Dis. 10 (2019) 612, https://doi.org/10.1038/s41419-019-1856-y.
[57] S. Xie, M. Chen, B. Yan, X. He, X. Chen, D. Li, Identification of a role for the PI3K/AKT/mTOR signaling pathway in innate immune cells, PLoS One 9 (2014), e94496, https://doi.org/10.1371/journal.pone.0094496.
[58] J. Tian, X. Zhang, H. Wu, C. Liu, Z. Li, X. Hu, S. Su, L.-F. Wang, L. Qu, Blocking the PI3K/AKT pathway enhances mammalian reovirus replication by repressing IFN-stimulated genes, Front. Microbiol. 6 (2015), https://doi.org/10.3389/fmicb.2015.00886.
[59] M. Utsugi, K. Dobashi, A. Ono, T. Ishizuka, S. Matsuzaki, T. Hisada, Y. Shimizu, T. Kawata, H. Aoki, Y. Kamide, M. Mori, PI3K p110β positively regulates lipopolysaccharide-induced IL-12 production in human macrophages and dendritic cells and JNK1 plays a novel role, J. Immunol. 182 (2009) 5225–5231, https://doi.org/10.4049/jimmunol.0801352.
[60] S.K. Polumuri, V.Y. Toshchakov, S.N. Vogel, Role of phosphatidylinositol-3 kinase in transcriptional regulation of TLR-induced IL-12 and IL-10 by fcγ receptor ligation in murine macrophages, J. Immunol. 179 (2007) 236–246, https://doi.org/10.4049/jimmunol.179.1.236.